



HAL
open science

Use of the breeding technique to estimate the structure of the analysis "errors of the day"

M. Corazza, E. Kalnay, D. J. Patil, S.-C. Yang, R. Morss, M. Cai, I. Szunyogh, B. R. Hunt, J. A. Yorke

► **To cite this version:**

M. Corazza, E. Kalnay, D. J. Patil, S.-C. Yang, R. Morss, et al.. Use of the breeding technique to estimate the structure of the analysis "errors of the day". *Nonlinear Processes in Geophysics*, 2003, 10 (3), pp.233-243. hal-00302201

HAL Id: hal-00302201

<https://hal.science/hal-00302201>

Submitted on 18 Jun 2008

HAL is a multi-disciplinary open access archive for the deposit and dissemination of scientific research documents, whether they are published or not. The documents may come from teaching and research institutions in France or abroad, or from public or private research centers.

L'archive ouverte pluridisciplinaire **HAL**, est destinée au dépôt et à la diffusion de documents scientifiques de niveau recherche, publiés ou non, émanant des établissements d'enseignement et de recherche français ou étrangers, des laboratoires publics ou privés.

Use of the breeding technique to estimate the structure of the analysis “errors of the day”

M. Corazza^{1,2}, E. Kalnay¹, D. J. Patil¹, S.-C. Yang¹, R. Morss³, M. Cai¹, I. Szunyogh¹, B. R. Hunt¹, and J. A. Yorke¹

¹University of Maryland, College Park, MD 20742-2425, USA

²INFM, Dipartimento di Fisica, Università di Genova, Italy

³NCAR, Boulder, Colorado, USA

Received: 3 April 2002 – Revised: 31 July 2002 – Accepted: 14 September 2002

Abstract. A 3D-variational data assimilation scheme for a quasi-geostrophic channel model (Morss, 1998) is used to study the structure of the background error and its relationship to the corresponding bred vectors. The “true” evolution of the model atmosphere is defined by an integration of the model and “rawinsonde observations” are simulated by randomly perturbing the true state at fixed locations.

Case studies using different observational densities are considered to compare the evolution of the Bred Vectors to the spatial structure of the background error. In addition, the bred vector dimension (BV-dimension), defined by Patil et al. (2001) is applied to the bred vectors.

It is found that after 3–5 days the bred vectors develop well organized structures which are very similar for the two different norms (enstrophy and streamfunction) considered in this paper. When 10 surrogate bred vectors (corresponding to different days from that of the background error) are used to describe the local patterns of the background error, the explained variance is quite high, about 85–88%, indicating that the statistical average properties of the bred vectors represent well those of the background error. However, a subspace of 10 bred vectors corresponding to the time of the background error increased the percentage of explained variance to 96–98%, with the largest percentage when the background errors are large.

These results suggest that a statistical basis of bred vectors collected over time can be used to create an effective constant background error covariance for data assimilation with 3D-Var. Including the “errors of the day” through the use of bred vectors corresponding to the background forecast time can bring an additional significant improvement.

Hollingsworth, 2002). This is due mostly to improvements in the models and in the method whereby atmospheric observations are incorporated into the initial conditions of the models, a process known as data assimilation (Daley, 1993; Kalnay, 2002). Most operational centers use a method called 3-Dimensional Variational data assimilation (3D-Var) to create the analysis that is used as an initial condition for the model. This method is a statistical interpolation of a short range forecast (typically 6 or 12 h) which serves as first guess or background, and the new observations. In this statistical interpolation, the background error covariance is maintained constant. That is, there is no accounting for the variations of the atmospheric state and consequent day-to-day variability of the background error covariance of forecasts from those states. These errors, not accounted by the fixed state of the background covariance matrix, are hereafter referred to as the “errors of the day”. The importance of the “errors of the day” can be seen in Fig. 1. Plotted is the root mean square analysis increment for the NCEP 50 year reanalysis during 1996, over two data-rich regions: the western (open circles) and eastern (gray dots) portions of the US. The average analysis increment (the correction introduced by the new observations) is about 8 m at 500 hPa, but it varies widely from day-to-day, between low values of less than 3 m to high values over 20 m.

There are several methods that try to account for the “errors of the day” in the forecast error covariance, including 4D-Var, Kalman Filtering, ensemble Kalman Filtering and the method of representers (e.g. Klinker et al., 2000; Bennett et al., 1996; Houtekamer and Mitchell, 1998; Hamill and Snyder, 2000). Unfortunately, these methods are computationally very expensive, and can only be implemented with substantial short-cuts, such as the use of a reduced rank background error covariance matrix in Kalman Filtering and lower model resolution in 4D-Var.

Kalnay and Toth (1994) argued that the similarity between breeding (Toth and Kalnay, 1993, 1997) and data assimilation suggests that the background errors should have a structure similar to those of bred vectors, but this conjecture has never been comprehensively tested. To test the validity

1 Introduction

Numerical weather prediction has made major progress in the last two decades (e.g. Kalnay et al., 1998; Simmons and

Correspondence to: E. Kalnay (ekalnay@atmos.umd.edu)

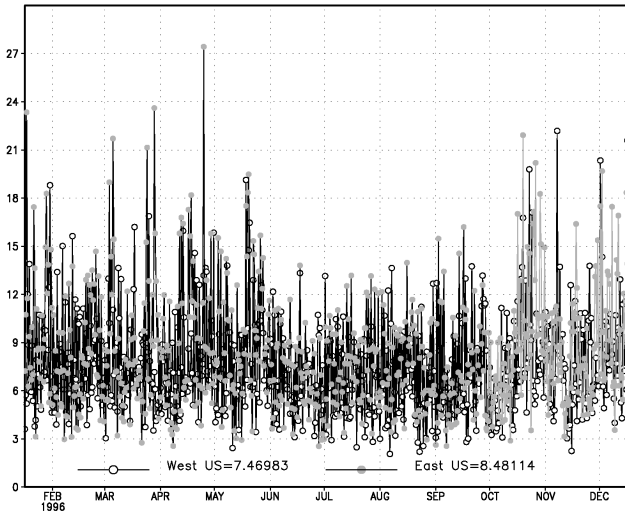


Fig. 1. Root mean square analysis increment in the 500 mb geopotential height for the NCEP 50 year reanalysis during 1996 over the western (open circles) and eastern (gray dots) portions of the US, courtesy of B. Kistler.

of this argument, a 3D-variational data assimilation scheme for a quasi-geostrophic channel model described in Morss (1998) and Rotunno and Bao (1996) is used to study the structure of the background error and its relationship to the corresponding bred vectors. The purpose of this paper is to test the extent to which bred vectors describe the shape of the “errors of the day”, and therefore could be used to include their effect in data assimilation, for example by augmenting the constant forecast error covariance used in 3D-Var with bred vectors (Corazza et al., 2002) or by performing an efficient local ensemble Kalman Filtering (Ott et al., 2002).

In Sect. 2, the quasi-geostrophic model and data assimilation system are reviewed and the method used to create bred vectors is presented. In Sect. 3 we first discuss the properties of the bred vectors and present qualitative comparisons of their structure with the background “errors of the day” for a single case. In Sect. 4 we present statistics that summarize the results over many cases. A summary and conclusions are presented in Sect. 5.

2 Experimental set-up

The numerical model is a non-linear quasi-geostrophic mid-latitude flow in a channel discretized by finite differences both in horizontal and vertical directions (Rotunno and Bao, 1996; Morss, 1998; Morss et al., 2001). Each level consists of a grid of 64 longitude and 32 latitude points with a grid size of roughly 250 km in both zonal and meridional directions. The model has seven levels, with five interior levels describing the evolution of potential vorticity; while potential temperature is represented at the upper and the lower boundaries. Horizontal diffusion is assumed to be proportional to

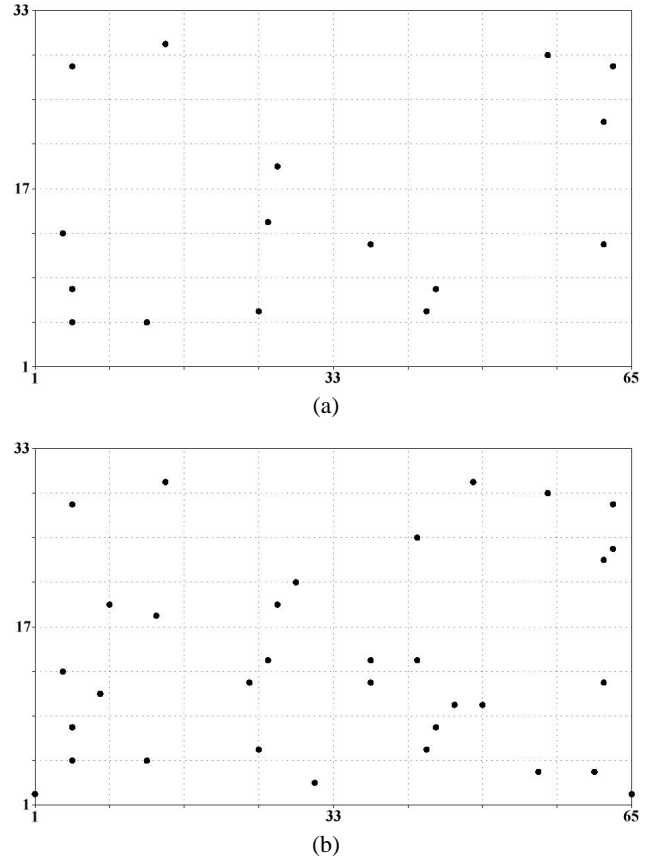


Fig. 2. Horizontal distribution of the rawinsonde locations for (a) the 16 stations experiments and (b) the 32 stations experiments.

the squared Laplacian, and the model is forced by relaxation to a zonal mean state (Hoskins and West, 1979).

As in Morss (1998) and Hamill et al. (2000), we chose a single model integration as the “true” evolution of the model atmosphere. “Rawinsonde observations” are generated every 12 h by randomly perturbing the true state at fixed observation locations (which were randomly chosen at initialization). Two different resolutions for the observation network (16 and 32 locations, respectively) have been used based on Morss (1998) results that indicate that these numbers of stations are representative of a low and medium density observing network, respectively. In Figs. 2a and b the observation locations for the two cases are shown. In order to avoid errors due to interpolation processes, measurements are taken at the model grid points. For every rawinsonde, values for temperature T and horizontal components of wind velocity u and v are simulated for all the seven layers of the model. The random noise to generate the observation errors is consistent using an observation-error covariance matrix which is set to zero except for variances and vertical covariances. The vertical correlation values are obtained by adapting the rawinsonde variances given in Parrish and Derber (1992) and using the vertical correlations given in Eq. (3.19) from Bergman (1979) (Morss, 1998).

The simulated data assimilation is performed with an al-

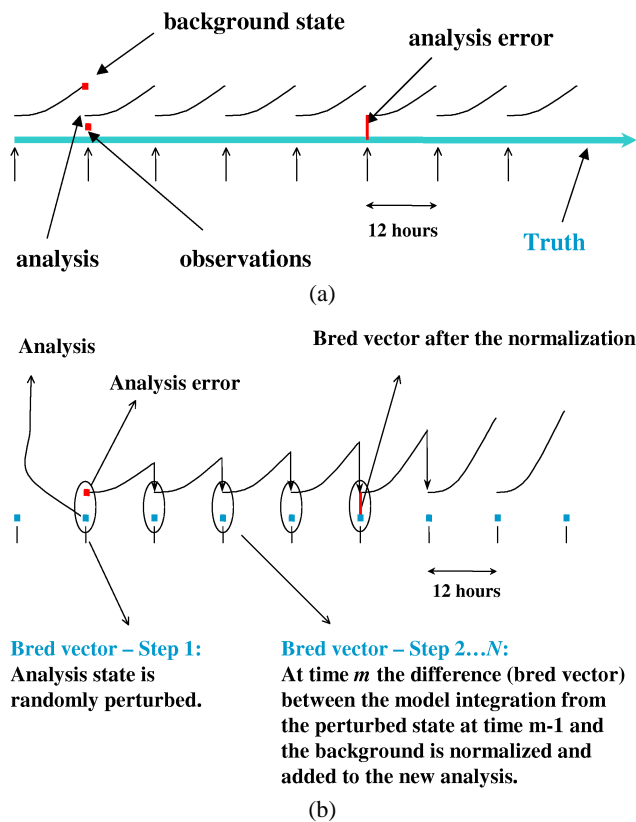


Fig. 3. (a) Schematic of the analysis cycle used in the system. Analysis times are indicated by the short vertical arrows. (b) Schematic of the method used for the generation of the bred vectors.

gorithm similar to the operational Spectral Statistical Interpolation (SSI) at NCEP (Parrish and Derber, 1992), which is a 3-D Var data assimilation scheme. In our experiments the same model is used for generating the truth and the forecasts, an approach known as a perfect model scenario (Fig. 3a). Because this is a simulation system in which the truth is known, it allows for the explicit computation of the analysis and background errors. The background-error covariance matrix \mathbf{B} is computed with the “NMC method”, deriving it from an ensemble of forecast differences, and assuming that \mathbf{B} is fixed in time and diagonal in horizontal spectral coordinates (as in Parrish and Derber, 1992). Moreover separate horizontal and vertical structures and simple vertical correlations are assumed. See Morss (1998) for more details on the implications of these assumptions and for a complete description of the implementation of the Data Assimilation System.

We compute k bred vectors in a manner similar to the procedure used in the ensemble forecasting systems at the National Centers for Environmental Prediction (Toth and Kalnay, 1993, 1997). The outline of the procedure is (Fig. 3b): (a) k random fields are added to the analysis; (b) the model is integrated for 12 h for each of the k perturbed fields; (c) the difference between each of the k perturbed integrations and the background 12 h forecast is uniformly scaled down so that the root mean square of the perturbation

is equal to the average squared analysis error at level three; (d) the k rescaled fields are then added to the new analysis and the steps (b) through (d) are repeated.

3 Characteristics of the bred vectors

Toth and Kalnay (1993, 1997) developed the breeding method to mimic in a simple way the data assimilation cycle, as suggested by a comparison of Figs. 3a and b. In an optimal sequential data assimilation scheme, the analysis error covariance is given by the forecast error covariance multiplied by a matrix $[\mathbf{I} - \mathbf{KH}]$, the identity matrix minus the product of the effective filter gain and the observational operator (e.g. Ide et al., 1997). In breeding, this matrix is replaced by the identity times a constant scalar representing the inverse of the global growth rate of the bred vector during the interval between rescalings. Kalnay and Toth (1994) conjectured that because of this similarity between the construction of the bred vectors and the data assimilation system both the background errors and the bred vectors would have similar local structures. In a perfect data assimilation system that accounts exactly for the errors of the day the conjecture may not be valid. For imperfect systems such as 3D-Var, if the background errors dominate the analysis errors, the conjecture is more plausible, but it needs to be experimentally verified, and a simulation system provides the best tool for this purpose.

In this section we qualitatively explore this conjecture and other issues related to the robustness and representativeness of the bred vectors after a finite transient. More quantitative results based on a local analysis and statistical comparisons with surrogate experiments are presented in Sect. 4.

When the “errors of the day” are large with respect to their average, both in simplified and the operational systems, they are dominated by the background errors (e.g. Fig. 7 in Szunyogh et al., 2000). Thus, it is of interest to compare the spatial structure of the bred vectors to that of the background error. It is the background error that is most relevant for data assimilation, since the background error covariance determines the characteristics of the assimilation. Figures 4a and b show a typical example of the midlevel background error of potential vorticity (contours) against two arbitrarily chosen bred vectors (shaded), at an arbitrarily chosen time, 36 days after initialization of the bred vectors. These results were obtained for a very low observation density (16 stations) simulation. There is a qualitative resemblance between the background error and the bred vectors. The contour and colored patterns shown in Fig. 4 are in good agreement in some areas (e.g. the prominent structure between point 10 and point 30 in the x axis and point 5 and point 25 in the y axis in Figs. 4a and 4b), but agree less well in other areas. For enhanced visualization, the contour lines of both the background error and of the bred vectors are shown in Fig. 4c. Figure 4d shows plots of the quantities represented in Fig. 4c for one dimensional slices at $y = 10$. Again the similarity between the two bred vectors and the background error is evident over regions

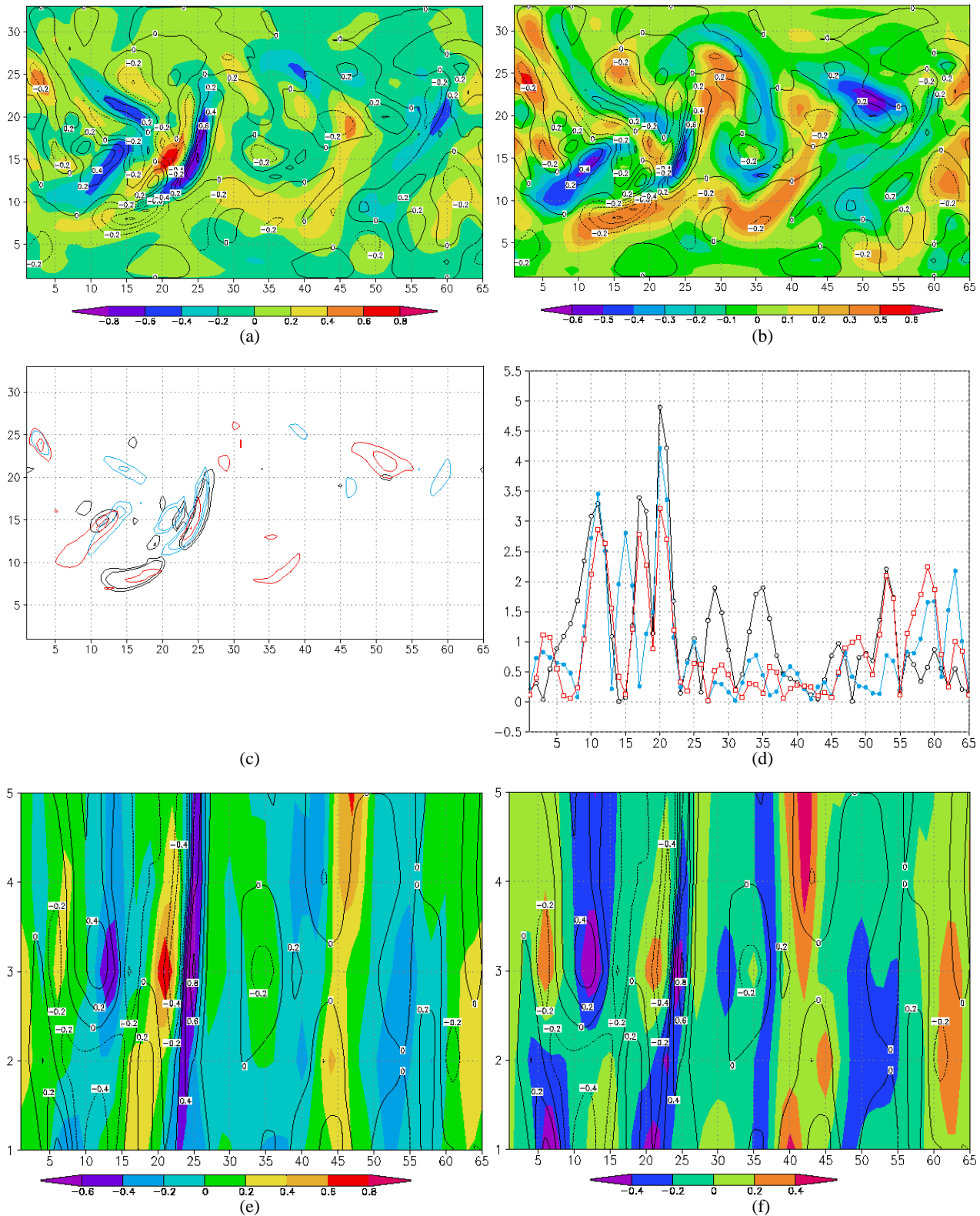


Fig. 4. (a) and (b) potential vorticity (color) at level three for two randomly chosen bred vectors after 36 days for a low density observing network (16 rawinsondes). Contours represent the background error. (c) background error (black) and bred vectors shown in (a) and (b) (blue and red, respectively) normalized by their root mean square; contour lines are for the values 2.3 and 3. (d) vertical cross-section of the same vectors of (c) [$y = 15$]. (e) and (f) same as (a) and (b) but vertical cross-section for $y = 15$.

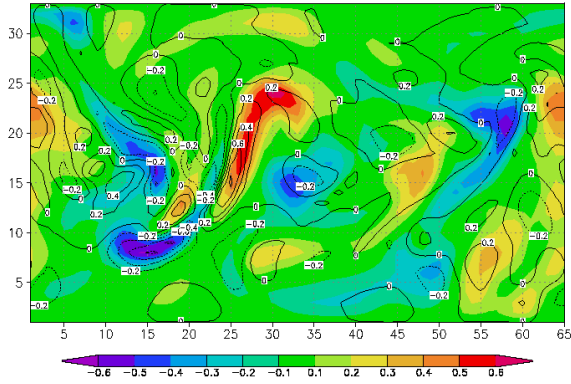


Fig. 5. Background error (contour) and a bred vector (color shaded) obtained with a breeding cycle based on the truth. The figure should be compared with Figs. 4a and b where the breeding cycle is based on the analysis.

with large amplitudes. The conclusions shown for the horizontal structure are equally valid for the vertical structure. In the examples shown in Figs. 4e and f the structure of the error in the potential vorticity over most of the domain is well described by the bred vectors; nevertheless, in some areas it is possible to see secondary maxima in the bred vectors that do not correspond to any signal in the background error and vice versa.

3.1 Sensitivity to the details of the background flow

It has been questioned in the past whether bred vectors computed using the analysis (which is only an estimate of the truth) are representative of the bred vectors that would be obtained if they were computed as perturbations of the “true” atmosphere. The results for the quasi-geostrophic system (Fig. 4) show that bred vectors obtained from the analysis are indeed very similar to those obtained from the truth. Moreover, these results are valid for both low observational density (Fig. 4) and at higher observation density (Fig. 6). In Fig. 6 level 3 potential vorticity from the bred vectors number 1 and 5 and the background error are shown for the 32 stations simulation. As in the case of lower observational density, there is a good correspondence between the fields, and the structure of both the background error and the bred vector are similar to those obtained for the 16 observations simulation. This suggests that the analysis provides sufficiently close “shadowing” of the true atmosphere, and that the bred vectors depend on the instabilities of the large scale flow-of-the-day, rather than on the smaller scales details.

3.2 Finite time convergence

Toth and Kalnay (1993, 1997) observed for the operational global model of NCEP that it took only a transient period of few days for the randomly initialized bred vectors to develop well organized spatial structures in the mid-latitudes. This has been confirmed with the quasi-geostrophic model system: 3–5 days after initiating the breeding process with ran-

dom perturbations, the bred vector growth rates attain their typical asymptotic range of values, and the bred vectors develop structures similar to the background errors. This is in good agreement with the results of Reynolds and Errico (1999), who computed finite time estimates of the Lyapunov vector in a quasi-geostrophic atmosphere on the sphere (here the growth over an analysis period is taken as the inverse of the rescaling factor employed for the bred vector at the analysis time). This is shown in Fig. 7, which compares a bred vector (color shaded) and the background error (contours) five days after initiating the breeding process, and in Fig. 12, in the next section, which shows the rate at which convergence takes place.

3.3 Robustness with respect to the choice of norm

Because of their close relationship with leading Lyapunov vectors (Legras and Vautard, 1996; Szunyogh et al., 1997; Trevisan and Pancotti, 1998), bred vectors are expected to be insensitive to the choice of norm used to define the growth and rescaling. Figures 6 and 8 compare bred vectors obtained using a potential enstrophy (vorticity squared) norm,

$$\|\Delta q\| = \sqrt{\frac{1}{N} \sum_{i=1}^N (\Delta q)_i^2},$$

where $(\Delta q)_i$ is the difference in potential vorticity at the considered grid point i and N is the number of points, and a stream function norm,

$$\|\Delta \psi\| = \sqrt{\frac{1}{N} \sum_{i=1}^N (\Delta \psi)_i^2},$$

where $(\Delta \psi)_i$ is the difference in streamfunction at the grid point i . Bred vectors obtained with both norms show a similar shape and relationship to the background error. This allows us to present our results only for the potential vorticity norm without losing generality in the conclusions.

These results are in contrast with singular vectors, which are extremely sensitive to the choice of norm. Palmer et al. (1998) and Snyder and Joly (1998) have shown that singular vectors obtained with a squared streamfunction norm have a horizontal scale much smaller than that obtained using an enstrophy norm, and those obtained with an energy norm have intermediate scales.

4 Local analysis of the subspace of the bred vectors and its relationship to the background error

In this section we present a local analysis of the bred vectors that allows a quantitative comparison of the relationship between bred vectors and the background error.

4.1 Effective dimension of the bred vectors subspace

We define a local dimension of the bred vector space as in Patil et al. (2001). In the following we briefly describe this

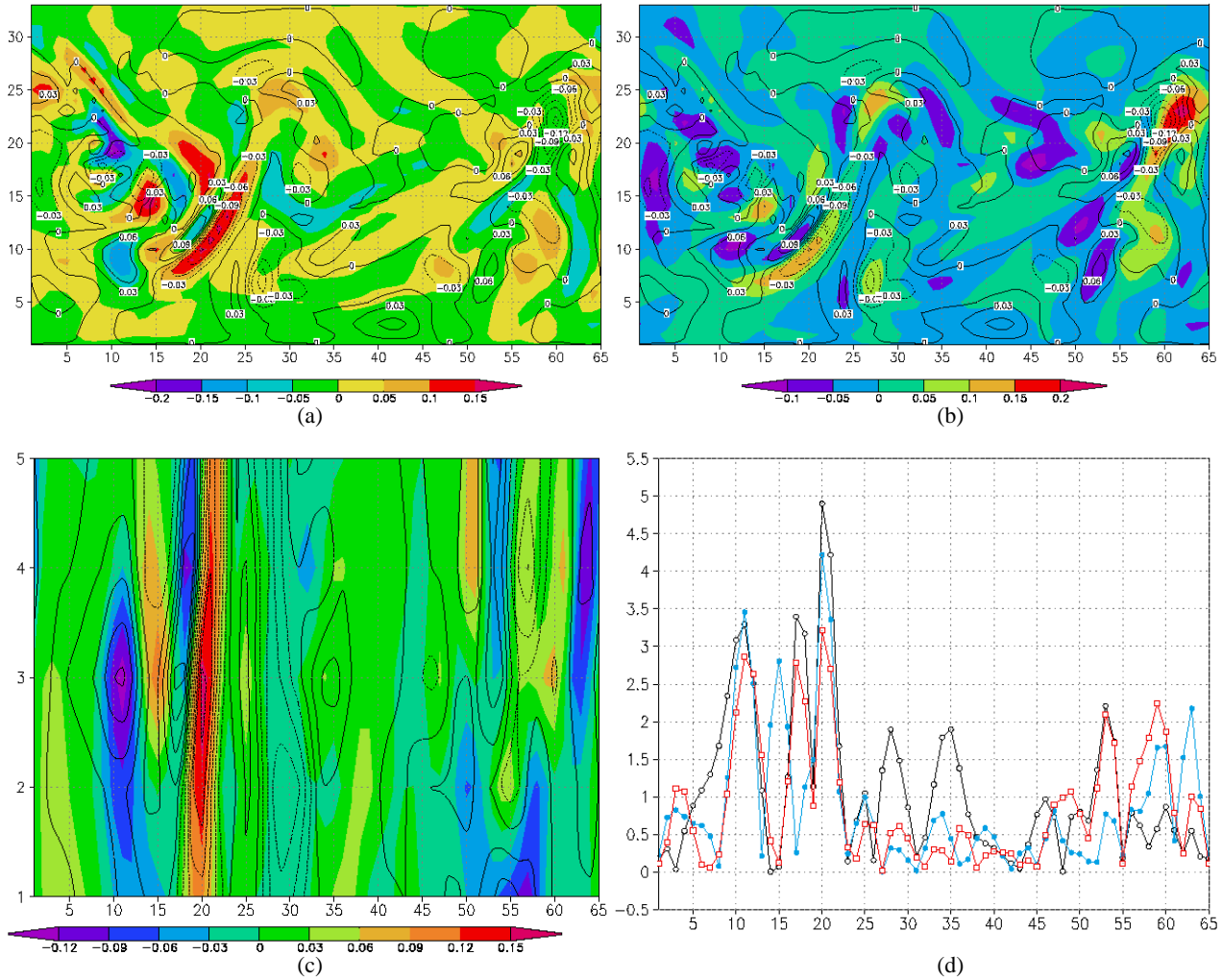


Fig. 6. (a) and (b) Two randomly chosen bred vectors for a medium density observing network (32 rawinsondes) (color shaded). Contours represent the corresponding background error. (c) vertical cross-section of the same vectors in (a) ($y = 10$). (d) same as Fig. 4d for the vectors represented in Figs. 6a and b [$y = 10$].

method. For every grid point a surrounding domain of 25 grid points (5×5) – the local domain – is considered. For every bred vector and every grid point, we consider the 25 dimensional vector composed of the values of potential vorticity over the grid points of the local domain, which we refer to as a local bred vector. If there are k bred vectors, then at any point there are k corresponding local bred vectors (in this section $k \leq 25$). We are interested in the degree of linear independence of the local bred vectors. That is, we want to determine a quantitative measure of the effective dimensionality of the subspace spanned by the k local bred vectors.

To do this Patil et al. (2001) use principal component analysis (Scheick, 1997) and define the bred vector dimension (BV-dimension) as:

$$\Psi(\sigma_1, \sigma_2, \dots, \sigma_k) = \frac{\left(\sum_{i=1}^k \sigma_i\right)^2}{\sum_{i=1}^k \sigma_i^2},$$

where σ_i , $i = 1, \dots, k$ are the singular values of the $k \times k$

covariance matrix of the $25 \times k$ matrix formed by the local vectors. In general this statistic returns a real value between 1 and k or 25, whichever is smaller. Note that while small perturbations due to noise or numerical error will typically cause the dimensionality of the space spanned by the k local vectors to be k , the effective dimension (BV-dimension) may be substantially lower and is robust to small changes in the σ_i due to noise or numerical error. Its relationship to the commonly used explained variance depends on the distribution of singular values. For example, if the squares of the two largest singular values are 0.9 and 0.05, (with a total explained variance of 95%) then the BV-dimension is close to 1; if they are 0.48 and 0.47, (total explained variance also 95%) then the BV-dimension is close to 2; if they are 0.47 and 0.46, (with a total explained variance of 93%) then the BV-dimension is still close to 2. In the first two cases, the number of singular vectors needed to explain 95% of the variance is 2, and in the third case it is at least 3. This simple example shows that although the BV-dimension is related to the number of vec-

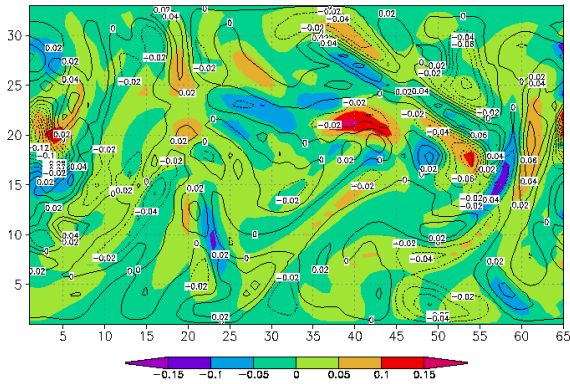


Fig. 7. A bred vector (color shaded) and background error (contour) in potential vorticity at midlevel after 5 days from its initialization using the potential vorticity norm for rescaling.

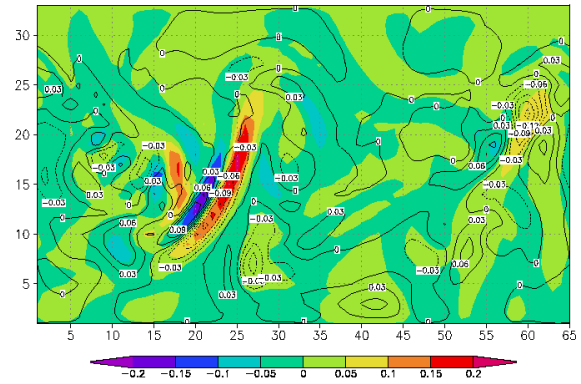


Fig. 8. Same as Figs. 6a or b but with the bred vector obtained using a streamfunction norm. Note that in Fig. 6 the bred vectors were obtained using potential vorticity norm.

tors needed to explain a certain level of variance, it has the advantage that, unlike explained variance, it is insensitive to the selection of an arbitrary threshold.

In our case we found that for $k = 10$ the local dimension of this subspace is always smaller than about 5, and that there are areas where the dimensionality is much lower (less than 3). In Fig. 9 an example of the bred vector dimension is shown for the midlevel potential vorticity using different numbers of bred vectors. It is seen that increasing the number of bred vectors beyond 10 yields only a small spatial changes in the BV-dimension, especially in the regions of low dimensionality. This indicates that the results obtained with the local analysis with a set of 10 bred vectors can be considered representative of larger numbers of bred vectors in regions of low dimensionality. A more detailed analysis can be found in Patil (2001).

Figure 10a shows a scatter plot with the BV-dimension obtained at every grid point using 10 bred vectors during a period of 90 days, versus the background error squared valid at the same point in space and time. The same plot is made for the BV-dimension using 10 surrogates (Theiler et al., 1992) of the bred vectors, i.e. bred vectors corresponding to randomly chosen times that are at least 10 days away from each other and from the background error, so as to remove any temporal correlation. The minimum and maximum BV-dimensions obtained on a daily basis with the real bred vectors has a mean of 1.4 and 3.7, respectively, whereas for surrogate vectors these values are about 4.2 and 7.5, respectively. The average BV-dimension of the surrogates, about 5.5, is low compared to the total subspace, but much larger than that obtained with bred vectors valid at the same time, which is 2.6. An analysis similar to that presented in Table 1 shows that (unlike explained variance), there is no significant dependence of the BV-dimension on the size of the background error.

Since bred vectors are computed using a finite time, finite amplitude extension to the method used to compute leading Lyapunov vectors, it might be expected that they should all converge to a single leading bred vector. However this is not

the case in the operational global forecast models or even for the simpler quasi-geostrophic model (Fig. 10a). This is due to nonlinear forcing and to the fact that in these complex systems several instabilities can coexist in different locations (Kalnay et al., 2002). As a result the bred vectors remain globally different, but in regions in which the background flow is locally unstable, they collapse into a lower-dimensional subspace represented by the dominant local instabilities.

4.2 Similarity between the local structure of bred vectors and background errors

In Sect. 3 we showed qualitative instantaneous similarity between individual bred vectors and the background errors. This similarity can be quantified by computing the extent to which the background error lies within the subspace of the bred vectors. At each point, for 90 days, we computed the local angle between the background error and the subspace of bred vectors, and therefore found that in most grid points the angle is less than 10° , corresponding to an explained variance (e.g. Wilks, 1995) of more than 0.97. Figure 11a shows a scatterplot of the explained variance (square of the angle between the background error and the subspace of 10 bred vectors) as a function of the background error size for a period of 90 days. It clearly shows that the background error is mostly confined to the subspace of the bred vectors and therefore that it is in principle possible to effectively correct the background state by simply moving it toward the observations within this subspace. Figure 11b shows the same scatterplot but for the surrogate bred vectors corresponding to 10 randomly chosen times, as in Fig. 10b. Table 1 summarizes the statistics for the explained variance. The t-test corresponds to the null hypothesis that the real bred vectors and the surrogates explain the same variance, and shows that it should be rejected with very high significance.

It is interesting to notice that although the surrogates provide a lower value of explained variance of the local pattern of the background error, they still explain over 85% of the

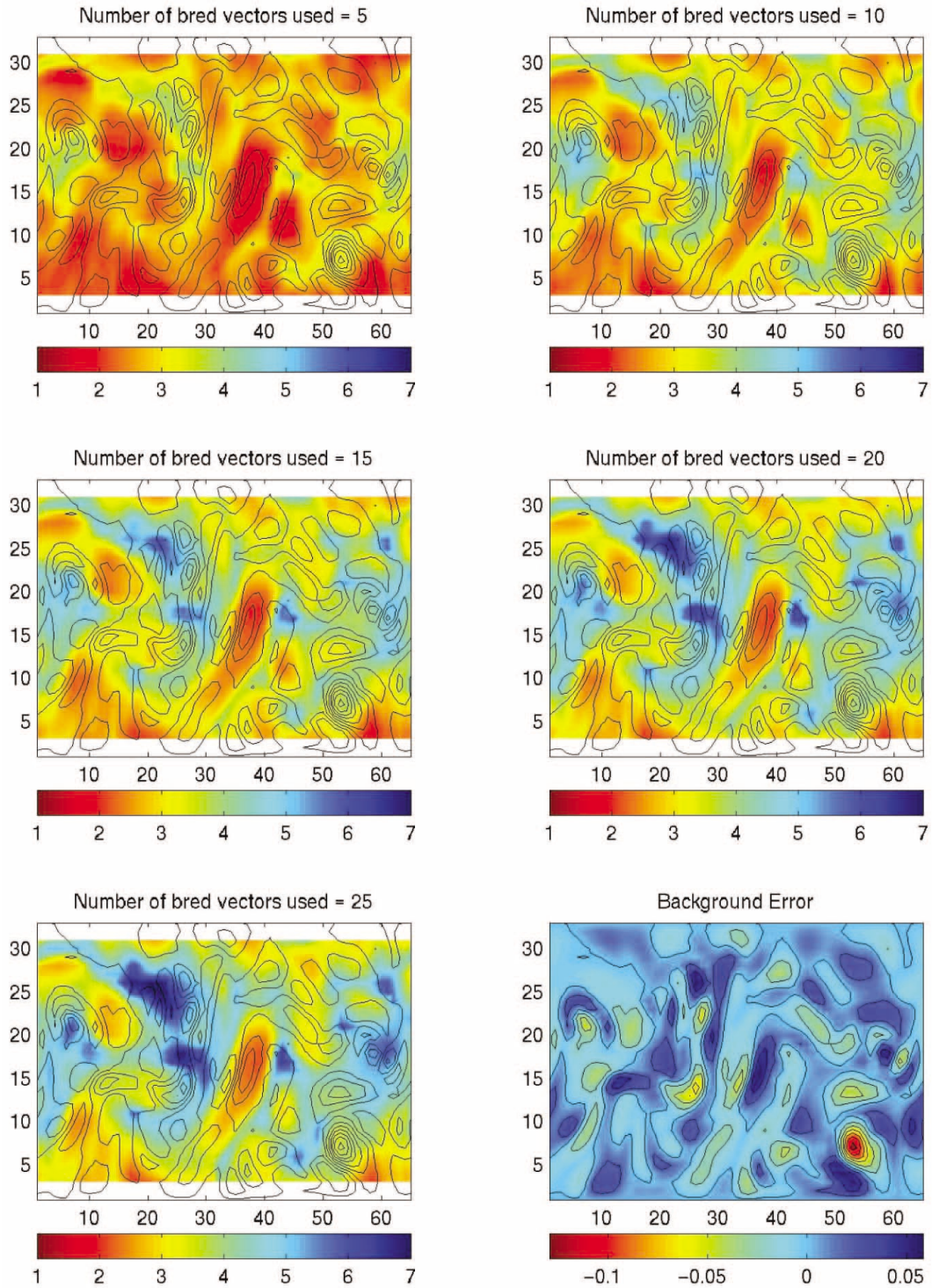


Fig. 9. BV-dimension (5×5 local domains) obtained using different numbers of bred vectors (5–25 vectors). The contour lines show the background error (also shown in color shades in the bottom-right plot).

variance, much better than what a subspace of random vectors would do. This should not be surprising, because, by construction, the surrogates are representative of the statistically averaged subspace of bred vectors. The construction of the 3D-Var background error covariance using the “NMC method” (Parrish and Derber, 1992) is based on a subspace

of vectors related to the surrogate bred vectors. It is obtained from the difference between forecasts verifying at the same time, which should be dominated by bred vectors, averaged over one or two months. Therefore we can consider Fig. 11b as a rough estimate of the projection of the background errors onto the subspace of vectors used in 3D-Var. Figure 11a

Table 1. Comparison of the explained variance of the background error using real bred vectors and surrogates (bred vectors corresponding to randomly chosen times). The results are computed for every grid point over 90 days, and binned as a function of the square of the background error

Background error squared		Explained Variance				
		Real BVs		Surrogate		test
range	% of points	Mean	STD	Mean	STD	T test
0.0–0.1	57.58	0.9608	0.0505	0.8519	0.1188	92.01
0.1–0.2	14.39	0.9678	0.0454	0.8648	0.1167	47.42
0.2–0.3	7.82	0.9723	0.0396	0.8730	0.1129	36.62
0.3–0.4	4.75	0.9756	0.0317	0.8620	0.1220	27.04
0.4–0.5	3.17	0.9761	0.0330	0.8674	0.1154	23.21
0.5–0.6	2.40	0.9759	0.0351	0.8675	0.1072	21.53
0.6–0.7	1.70	0.9746	0.0500	0.8711	0.1047	17.60
0.7–0.8	1.52	0.9814	0.0293	0.8693	0.1165	16.08
0.8–0.9	1.12	0.9789	0.0326	0.8800	0.1018	15.49
0.9–1.0	0.95	0.9797	0.0359	0.8652	0.1244	11.76
1.0–1.5	3.08	0.9831	0.0268	0.8810	0.1039	25.63
1.5–2.0	1.53	0.9819	0.0296	0.8804	0.1123	16.66

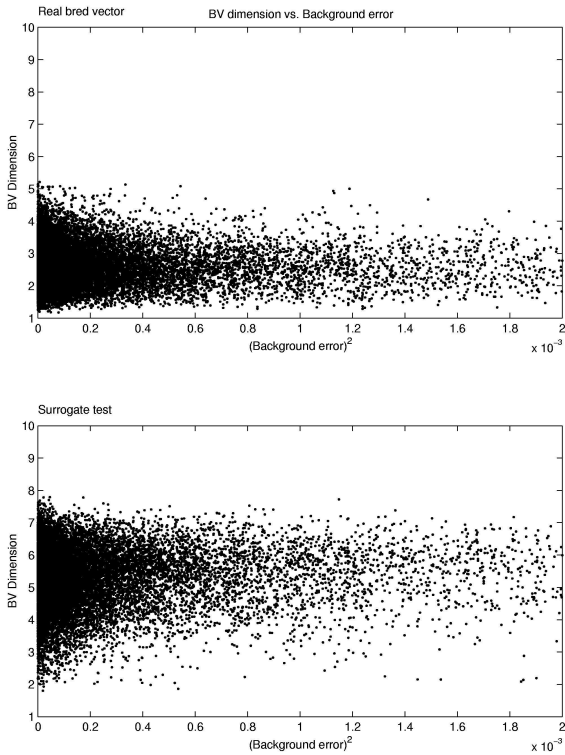


Fig. 10. BV-Dimension as a function of the background error squared, computed for 90 days over every grid point. (a) using 10 bred vectors corresponding to the same time as the background error. (b) using 10 surrogate bred vectors corresponding to random times.

shows the potential improvement that including the “errors of the day” could bring to the 3D-Var data assimilation.

Finally, in Fig. 12 we show the evolution of the average ex-

plained variance as a function of time for bred vectors started from initial random perturbations. It shows that the bred vector subspace converges quickly, within 3–5 days, and that the results are robust in time. For the surrogates the explained variance does not change with time.

5 Discussion and conclusions

In this paper we have used a 3D-variational data assimilation scheme for a quasi-geostrophic channel model (Morss, 1998) to study the structure of the background error and its relationship to the corresponding bred vectors. By defining a model integration as the “true” evolution of the model atmosphere we were able to explicitly compute the background errors and make direct comparisons of these errors to bred vectors. We have observed that in the quasi-geostrophic simulation system, as in the operational data assimilation system, the background errors have a large day-to-day variability, which we have called “errors of the day”. The errors of the day tend to have periods of fast growth, resulting in large amplitudes intermittent in both space and in time.

We have obtained the following results:

- Convergence to well organized structures in the bred vectors occurs within a few (3–5) days (Sects. 3.2 and 4.2).
- Bred vectors obtained using normalizations based on the potential vorticity and on the streamfunction have very similar structures (Sect. 3.3).
- Bred vectors obtained using the “true” atmosphere are very similar to those obtained using the “analysis” atmosphere (Sect. 3.1). This is true whether we use a high or low density observing network, suggesting that

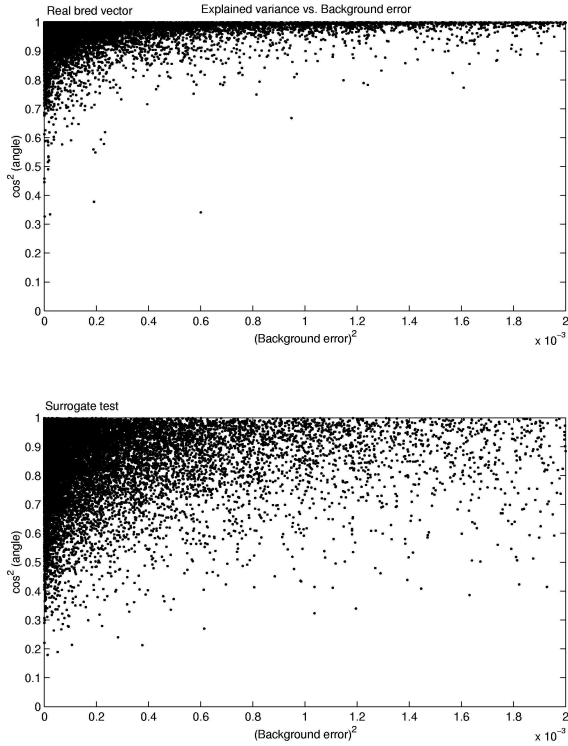


Fig. 11. Explained variance (square of the cosine of the angle between the background error and the space defined by the local vectors) as a function of the background error squared, computed for 90 days over every grid point. **(a)** using 10 bred vectors corresponding to the same time as the background error. **(b)** using 10 surrogate bred vectors corresponding to random times.

the bred vectors are not too sensitive to the details of the flow and that the errors themselves are more likely dependent on the large scale nature of the flow (at least in a perfect model assumption). Since the truth is not available in practice, this is important because it suggests that basing bred vectors on the analysis is not a significant limitation in operational systems.

- The bred vectors have spatial characteristics similar to those of the background “error of the day” (Figs. 4, 12).
- Following Patil et al. (2001) we computed a measure of the space spanned by the bred vectors (BV-dimension). We found that the local dimension is much smaller than the number of bred vectors. Moreover, the information given by a set of ten bred vectors is not significantly different from that obtained using a larger number of vectors (Sect. 4).
- We also defined the local angle between the forecast error and the subspace of bred vectors. When averaging over many cases, we found that in most of the model domain the angle is confined to less than 10° , with a mean explained variance of 96–98%, indicating that the background error is mostly confined to the subspace of the bred vectors (Sect. 4.2). Larger angles (lower explained

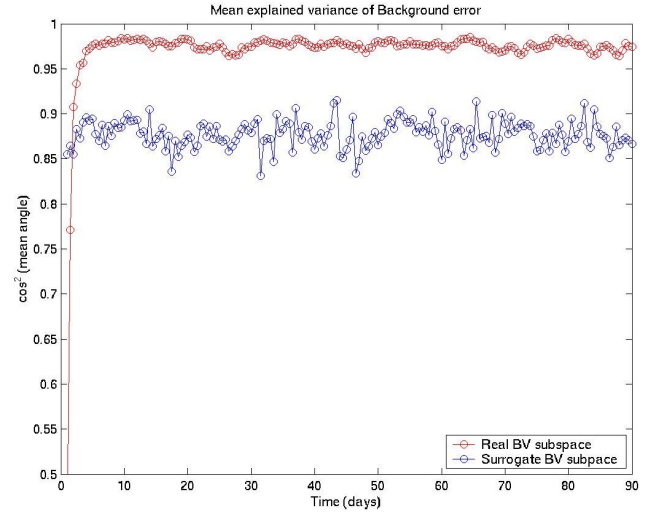


Fig. 12. Evolution of the average explained variance as a function of time for bred vectors started from initial random perturbations (red dots) and for the surrogate (blue line).

variance) are only observed in regions where the background error is small (Fig. 12).

- The explained variance of the forecast error using surrogate bred vectors (corresponding to random times) is also high, about 85%. We suggest that this reflects the reason why 3D-Var is quite successful even though it does not take into account the errors of the day, since the “NMC method” used to construct the background error covariance is based on forecast differences related to bred vectors.

These results suggest that the bred vectors can indeed be useful in specifying the part of the background error covariance that corresponds to the “errors of the day”. We are currently developing computationally inexpensive methods to take advantage of this information. Preliminary results (Corazza et al., 2002) indicate a substantial improvement in the analysis errors and in the forecasts at a small computational overhead. An economic local ensemble Kalman Filtering approach is described in Ott et al. (2002).

Finally, we point out that these results were obtained in the context of a perfect model, and we have not yet addressed the problem of model deficiencies. However, forecast experience with global models (e.g. Kalnay et al., 1998; Simmons and Hollingsworth, 2002; Reynolds et al., 1994) indicates that away from the tropics and for synoptic and larger scales, model errors are small compared with the “errors of the day” that grow due to the unstable dynamics, suggesting that in these areas bred vectors can indeed be used to improve data assimilation. We plan to assess the impact of model deficiencies by performing breeding with several different models.

Acknowledgements. The authors are grateful to E. Ott for his constant support and important contributions at every stage of the work. We would also like to thank the two anonymous reviewers whose

comments led to a major improvement in the paper. This research was supported by the W. M. Keck Foundation, NPOESS IPO (adaptive targeting, grant SWA01005), NASA (AIRS data assimilation, STMD CG0127), Office of Naval Research, and National Science Foundation (award DMS0104087, grant no. 0104087).

References

- Bennett, A. F., Chua, B. S., and Leslie, L. M.: Generalized inversion of a global NWP model, *Meteor. Atmos. Phys.*, 60, 165–178, 1996.
- Bergman, K. H.: Multivariate analysis of temperatures and winds using optimum interpolation, *Mon. Wea. Rev.*, 107, 1423–1444, 1979.
- Corazza, M., Kalnay, E., Patil, D. J., Ott, E., Yorke, J., Szunyogh, I., and Cai, M.: Use of the breeding technique in the estimation of the background error covariance matrix for a quasigeostrophic model, in *AMS Symposium on Observations, Data Assimilation and Probabilistic Prediction*, pp. 154–157, Orlando, Florida, 2002.
- Daley, R.: *Atmospheric data analysis*, Cambridge University Press, New York, 1993.
- Hamill, T. M. and Snyder, C.: A Hybrid Ensemble Kalman Filter-3D Variational Analysis Scheme, *Mon. Wea. Rev.*, 128, 2905–2919, 2000.
- Hamill, T. M., Snyder, C., and Morss, R. E.: A Comparison of Probabilistic Forecasts from Bred, Singular-Vector and Perturbed Observation Ensembles, *Mon. Wea. Rev.*, 128, 1835–1851, 2000.
- Hoskins, B. J. and West, N. V.: Baroclinic waves and frontogenesis. Part II: Uniform potential vorticity jet flows – Cold and warm fronts, *J. Atmos. Sci.*, 36, 1663–1680, 1979.
- Houtekamer, P. L. and Mitchell, H. L.: Data assimilation using an ensemble Kalman filter technique, *Mon. Wea. Rev.*, 126, 796–811, 1998.
- Ide, K., Courtier, P., Ghil, M., and Lorenc, A. C.: Unified notation for data assimilation: Operational, sequential, and variational, *J. Meteor. Soc. Japan*, 75(1B), 181–189, 1997.
- Kalnay, E.: *Atmospheric Modeling, Data Assimilation and Predictability*, Cambridge University Press, 340 pp., 2002.
- Kalnay, E. and Toth, Z.: Removing growing errors in the analysis cycle, in: *Tenth Conference on Numerical Weather Prediction*, pp. 212–215, Amer. Meteor. Soc., 1994.
- Kalnay, E., Lord, E. S., and McPherson, R.: Maturity of Operational Numerical Weather Prediction: the Medium Range, *Bull. Amer. Meteor. Soc.*, 79, 864–875, 1998.
- Kalnay, E., Corazza, M., and Cai, M.: Are bred vectors the same as Lyapunov vectors?, in: *AMS Symposium on Observations, Data Assimilation and Probabilistic Prediction*, pp. 173–177, Orlando, Florida, 2002.
- Klinker, E., Rabier, F., Kelly, G., and Mahfouf, J.-F.: The ECMWF operational implementation of four-dimensional variational assimilation, iii: Experimental results and diagnostics with operational configuration, *Quart. J. Roy. Meteor. Soc.*, 126, 1191, 2000.
- Legras, B. and Vautard, R.: A guide to Liapunov vectors, in *Proceedings 1995 ECMWF Seminar on Predictability, Vol I*, pp. 143–156, 1996.
- Morss, R. E., *Adaptive observations: Idealized sampling strategies for improving numerical weather prediction*, Ph.D. thesis, Massachusetts Institute of Technology, 225 pp., 1998.
- Morss, R. E., Emanuel, K. A., and Snyder, C.: Idealized Adaptive Observation Strategies for Improving Numerical Weather Prediction, *J. Atmos. Sci.*, 58, 210–234, 2001.
- Ott, E., Hunt, B. R., Szunyogh, I., Corazza, M., Kalnay, E., Patil, D. J., and Yorke, J. E.: Exploiting low-dimensionality of the atmospheric dynamics for efficient ensemble kalman filtering, <http://arXiv:physics/0203058/>, 2002.
- Palmer, T. N., Gelaro, R., Barkmeijer, J., and Buizza, R.: Singular vectors, metrics and adaptive observations, *J. Atmos. Sci.*, 55, 633–653, 1998.
- Parrish, D. F. and Derber, J. D.: The National Meteorological Center spectral statistical interpolation analysis system, *Mon. Wea. Rev.*, 120, 1747–1763, 1992.
- Patil, D. J.: *Applications of chaotic dynamics to weather forecasting*, Ph.D. thesis, University of Maryland, 2001.
- Patil, D. J. S., Hunt, B. R., Kalnay, E., Yorke, J. A., and Ott, E.: Local Low Dimensionality of Atmospheric Dynamics, *Phys. Rev. Lett.*, 86, 5878, 2001.
- Reynolds, C. A. and Errico, R. M.: Convergence of singular vectors toward Lyapunov vectors, *Mon. Wea. Rev.*, 127, 2309–2323, 1999.
- Reynolds, C. A., Webster, P. J., and Kalnay, E.: Random error growth in NMC’s global forecasts, *Mon. Wea. Rev.*, 122, 1281–1305, 1994.
- Rotunno, R. and Bao, J. W.: A case study of cyclogenesis using a model hierarchy, *Mon. Wea. Rev.*, 124, 1051–1066, 1996.
- Scheick, J. T.: *Linear Algebra with Applications*, McGraw Hill, 1997.
- Simmons, A. J. and Hollingsworth, A.: Some aspects of the improvement in skill of numerical weather prediction, *Quart. J. Roy. Meteor. Soc.*, 128, 2002.
- Snyder, C. and Joly, A.: Development of perturbations within a growing baroclinic wave, *Quart. J. Roy. Meteor. Soc.*, 124, 1961–1983, 1998.
- Szunyogh, I., Kalnay, E., and Toth, Z.: A comparison of Lyapunov and optimal vectors in a low resolution GCM, *Tellus*, 49A, 200–227, 1997.
- Szunyogh, I., Toth, Z., Morss, R. E., Majumdar, S. J., Etherton, B. J., and Bishop, C. H.: The Effect of Targeted Dropsonde Observations during the 1999 Winter Storm Reconnaissance Program, *Mon. Wea. Rev.*, 128, 3520–3537, 2000.
- Theiler, J., Eubank, S., Longtin, A., Galdrikian, B., and Farmer, J. D.: Testing for nonlinearity in time series: the method of surrogate data, *Physica D*, 58, 77–94, 1992.
- Toth, Z. and Kalnay, E.: Ensemble forecasting at NMC: the generation of perturbations, *Bull. Amer. Meteor. Soc.*, 74, 2317–2330, 1993.
- Toth, Z. and Kalnay, E.: Ensemble forecasting at NCEP: the breeding method, *Mon. Wea. Rev.*, 125, 3297–3318, 1997.
- Trevisan, A. and Pancotti, F.: Periodic orbits, Lyapunov vectors and singular vectors in the Lorenz system, *J. Atmos. Sci.*, 55, 390–398, 1998.
- Wilks, D. S.: *Statistical Methods in the atmospheric sciences*, Academic Press, New York, 1995.